Critical properties and Rényi entropies of the spin-$\frac{3}{2}$ XXZ chain

M. Dalmonte,[1,2,*] E. Ercolessi,[2] and L. Taddia[2,3,†]

[1]*Institute for Quantum Optics and Quantum Information of the Austrian Academy of Sciences, A-6020 Innsbruck, Austria*

[2]*Dipartimento di Fisica dell'Università di Bologna and INFN, via Irnerio 46, 40126 Bologna, Italy*

[3]*IFT UAM/CSIC, 28049 Cantoblanco, Madrid, Spain*

(Received 23 January 2012; published 6 April 2012)

We discuss entanglement and critical properties of the spin-3/2 XXZ chain in its entire gapless region. Employing density-matrix renormalization-group calculations combined with different methods based on level spectroscopy, correlation functions, and entanglement entropies, we determine the sound velocity and the Luttinger parameter of the model as a function of the anisotropy parameter. Then, we focus on entanglement properties by systematically studying the behavior of Rényi entropies under both open and periodic boundary conditions, providing further evidence of recent findings about entanglement entropies of excited states in conformal field theory.

DOI: 10.1103/PhysRevB.85.165112 PACS number(s): 75.10.Pq, 05.70.Jk, 05.10.Cc

I. INTRODUCTION

Since their first introduction,[1] quantum spin chains have been an incredibly fertile field for theoretical physicists. They are in fact interesting for various reasons: first of all because of their one-dimensional (1D) nature, which enhances the importance of quantum fluctuations and forbids the application of mean-field or other ordinary perturbative approaches; secondarily because of the integrability of some of them and the possibility of giving a description of their low-energy sector by means of effective quantum field theories; and lastly because of the availability of some numerical techniques that appear to be particularly powerful in these cases.

Spin-1/2 quantum spin chains with nearest-neighbor interactions[2,3] have been widely considered in literature and among them, the XXZ spin-1/2 chain is by far the most studied, both analytically and numerically. Being integrable via Bethe ansatz,[2] it represents a yardstick for nonexact techniques. Also, the physics of its low-energy sector is described in the continuum limit by a special class of conformal field theories (CFTs)[4,5] with conformal charge $c = 1$, the so-called Tomonaga-Luttinger liquids (TLLs)[6–8] which represent a paradigm for all those models whose excitations are of bosonic nature.[9,10]

Higher spin XXZ chains are also very interesting, because they constitute examples of models for which, despite being nonintegrable, one can provide quite well-known established field theory descriptions.[11,12] Moreover, their properties may be quantitatively determined with good accuracy by means of numerical simulations based on several efficient methods such as exact diagonalization, quantum Monte Carlo, and density-matrix renormalization group (DMRG).[10] Thus, they represent a decisively indicative and efficient test in order to establish the validity of properties that, up to now, have been verified mainly in integrable systems. In addition, the physics of these models can also be studied experimentally: for example, the spin-3/2 isotropic case is thought to model the behavior of some kind of quasi-1D antiferromagnets of magnetic ions, such as $CsVCl_3$ (Ref. 13) and $AgCrP_2S_6$,[14] whereas various spin models may now be engineered in cold matter setups of trapped ions[15–17] and have promising future implementation with ultracold atoms and molecules in strongly anisotropic optical lattices[18–21] and Rydberg atoms.[22]

In recent times, much attention has been devoted to the connection between quantum phase transitions and entanglement properties in strongly correlated systems.[23,24] In particular, whenever the effective theory describing a system is conformal, it is well known that a fruitful way to get physical information from numerical simulations, especially from DMRG[25,26] calculations, is to look at quantities known as Rényi entanglement entropies (REs).[27–31] More specifically, as will be recalled in the following, for TLLs the knowledge of the REs yields a very careful estimation not only of the central charge of the underlying critical theory,[32–34] but also of the decay exponents of correlation functions,[30,35,36] which are encoded in the so-called Luttinger parameter K.

The main aim of this work is to present a complete investigation of critical and entanglement properties of the $S = 3/2$ XXZ model over its gapless regime, and to compare the accuracy of different analysis methods employed to extrapolate thermodynamic quantities from finite-size numerical calculations based on the DMRG algorithm. In the first part, we will fully exploit the low-energy field theory of the XXZ model and determine its relevant quantities by considering different, independent observables; then, we will present an investigation of the entanglement entropies for bipartite intervals, considering both ground and excited states and systematically comparing the numerical findings with CFT predictions. The paper is structured as follows: in Sec. II, we briefly review the main features of spin-S XXZ chains from a field theoretical viewpoint, focusing on the TLL universality class emerging in the half-integer S case. We present our DMRG calculations and results on the $S = 3/2$ model in Sec. III, together with a brief resumé of all applied techniques. In Sec. IV, we perform a systematic investigation of the Rényi entropies of both the ground and excited states and compare the numerical findings with the predictions based on CFTs. Finally, we summarize the results and draw our conclusions in Sec. V.

II. MODEL HAMILTONIAN

The spin-S anisotropic Heisenberg model, also known as the XXZ chain, is described by the following

Hamiltonian:[2]

$$H_{XXZ} = \sum_{i=1}^{L} \left(S_i^x S_{i+1}^x + S_i^y S_{i+1}^y + \Delta S_i^z S_{i+1}^z \right), \qquad (1)$$

where $\vec{S}_i$ is a spin-S operator relative to the ith site and Δ is the anisotropy coefficient. Here, S can take positive half-odd-integer or integer values. In the simplest case $S = 1/2$, the model is integrable by Bethe ansatz,[2,3] it is critical for $|\Delta| \leqslant 1$, and in the interval $-1 < \Delta \leqslant 1$ its low-energy physics is effectively described by a conformal field theory with central charge $c = 1$.

The picture becomes more puzzling as one moves away from the integrable $S = 1/2$ case. At the isotropic point $\Delta = 1$, chains with integer spin display a finite gap, whereas in the half-integer case the system is gapless and still described by a $c = 1$ CFT, as has been proved in a series of analytical and numerical studies.[11,12,37–39] In such gapless regime, which persists in the finite range of interactions $-1 < \Delta \leqslant 1$, the low-energy spectrum is universally described by a TLL Hamiltonian:[6–10]

$$H = \frac{v_s}{2\pi} \int dx [(\partial_x \vartheta)^2 / K + K(\partial_x \varphi)^2], \qquad (2)$$

where ϑ and φ are conjugated density and phase bosonic fields, while the two interaction-dependent parameters v_s and K are called sound velocity and Luttinger parameter, respectively. Both the long-distance decay of correlation functions and spectral properties are determined by v_s and K; however, since no exact solution is known except for $S = 1/2$, one has to resort to unbiased numerical methods in order to quantitatively estimate the dependence of such parameters with respect to Δ. For the $S = 3/2$ case, which we are going to extensively study in the following, various numerical studies have been reported in literature, based on both exact diagonalization of small systems[38] and simulations based on the DMRG algorithm;[29,36,39] we will systematically refer to and compare our results to the known ones in the remainder of the paper.

III. NUMERICAL RESULTS: CRITICAL PROPERTIES

In this section, we provide a complete study of the quantum critical regime $-1 < \Delta \leqslant 1$ for the $S = 3/2$ XXZ model employing the DMRG technique, which allows one to estimate both ground-state and excited-state properties with notable accuracy. Being interested in various physical quantities such as entropies, correlation functions, and spectral properties, we employ simulations with both open (OBC) and periodic (PBC) boundary conditions. While the former guarantee better accuracy in the DMRG procedure, the latter are not affected by boundary effects; providing estimates in both configurations represents a good check for our final results. In order to accurately determine all relevant quantities of interest, we perform calculations with up to 512 (1156) states per block for OBC (PBC), together with up to five sweeps for each intermediate size during the infinite-size algorithm; in such a setting, typical discarded weights are of order 10^{-8} (10^{-6}) during the last iteration.

Reliable estimates of the relevant physical quantities v_s and K may be obtained with different numerical analysis. In the following, we will employ three alternative methods based on independent quantities: energy scaling in the low-energy spectrum, entanglement entropy, and spin fluctuations. A detailed account on how such quantities are related to the sound velocity and the Luttinger parameter is given in each of the following sections.

A. Central charge

As a first step in our study, we extract the central charge of the system from the scaling of the block von Neumann entropy (VNE), which is defined as

$$S_1(l, L) = -\mathrm{Tr}_A \rho_A \log_2 \rho_A. \qquad (3)$$

Here, the system of total length L is bipartite in two subsystems A, B of length $l, L - l$, respectively, and ρ_A denotes the reduced density matrix of A with respect to B. In a CFT, one has[32,33,35]

$$S_1(l, L) = \frac{c}{3\eta} \log_2[L \sin(\pi l/L)/\pi] + s_1 + S_1^{\mathrm{osc}}, \qquad (4)$$

where the coefficient $\eta = 1, 2$ for PBC/OBC, s_1 is a model-dependent constant, and S_1^{osc} represents finite-size oscillating corrections.[35] In a finite system under PBC, the central charge can be determined by fitting the half-lattice entropy

$$S_1(L/2, L) = \frac{c}{3} \log_2(L/\pi) + s_1 \qquad (5)$$

as a function of the system size L by assuming a scaling form of the type $c(L) = c_0 + a_0 L^{a_1}$. Typical results are plotted in Fig. 1: a best fit of Eq. (5) for $L \in [28, 60]$ gives excellent agreement with the expected value, as $c_0 = 1.00$ up to a 2% error over the entire parameter range; for negative values of Δ, even better agreement is reached. Alternative techniques to extract c via finite-size scaling[27,29] lead to comparable results. A good estimate of the central charge represents a reliable check of our numerical calculations, and is also required to consistently perform a level spectroscopy analysis without targeting excitations in momentum space.[29,39]

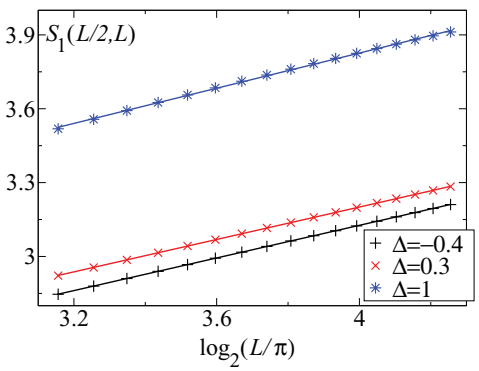

FIG. 1. (Color online) Finite-size scaling of the bipartite von Neumann entropy as a function of the system size $L \in [28, 60]$ for different values of the anisotropy coefficient Δ. Here, PBC are considered in order to discard oscillatory corrections. Solid lines represent fits with Eq. (5) yielding $c = 0.995(4)$, $0.992(6)$, and $1.014(4)$ from top to bottom.

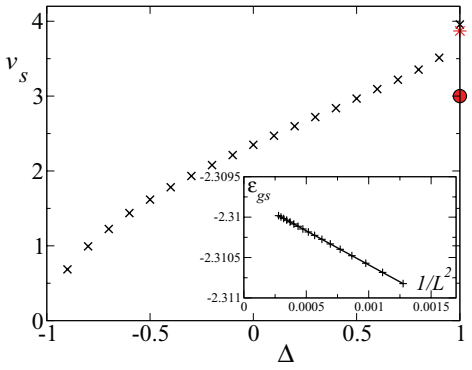

FIG. 2. (Color online) Sound velocity v_s as a function of Δ as extracted from level spectroscopy methods (black crosses); at $\Delta = 1$ the red circle denotes the spin-wave results $v_s = 3$, and a previous DMRG estimate (Ref. 39) $v_s = 3.87$ is indicated by a red star. The maximum error is of order $6 * 10^{-2}$ at the antiferromagnetic point. Inset: typical finite-size scaling of the ground-state energy density $\epsilon_{gs}(L)$ for $\Delta = -0.5$.

B. Sound velocity

Following standard level spectroscopy methods based on the energy scaling of CFTs,[5,29] the sound velocity v_s of the single-component TLL can be estimated by considering the finite-size scaling of the ground-state energy density, which under PBC reads as

$$\epsilon_{gs}(L) = \epsilon_0 + \frac{v_s c \pi}{6L^2} + \cdots, \tag{6}$$

ϵ_0 being the energy density in the thermodynamic limit, and employing the previously found values of the central charge. The large number of system sizes considered in our calculations allows one to safely perform a four-parameter fit of the form $\epsilon_{gs}(L) = a_0 + a_1/L^2 + a_2/L^{a_3}$; typical fitting results are shown in the inset of Fig. 2. At the antiferromagnetic point $\Delta = 1$, our results are in good agreement with a previous DMRG study,[39] where v_s was extracted by targeting the first excited states at finite momentum, and in sharp disagreement with the spin-wave result,[40] $v_s^{SW} = 3$, in which quantum fluctuations are only approximately treated. Including logarithmic corrections according to the Wess-Zumino-Novikov-Witten[9,39] theory does not lead to appreciable differences.

The complete dependence of v_s versus Δ is plotted in Fig. 2 and suggests how, once approaching the ferromagnetic phase transition, the velocity of the sound excitations seems to approach zero. On the other hand, v_s reaches its maximum value at the Berezinskii-Kosterlitz-Thouless point,[9] in full analogy with the $S = 1/2$ case.[3,9]

C. Luttinger parameter

When dealing with models whose low-energy physics is captured by the TLL Hamiltonian, the parameter K represents a fundamental quantity as it determines the long-distance decay of all correlation functions and thus which susceptibilities are the most relevant in the microscopic model.[10] We will thus employ three complementary methods to extract such a quantity from numerical simulations. This procedure allows one to systematically check the validity of each method in various parameter regimes and, close to the antiferromagnetic point, indicates which type of estimate is more affected by the well-known logarithmic corrections.

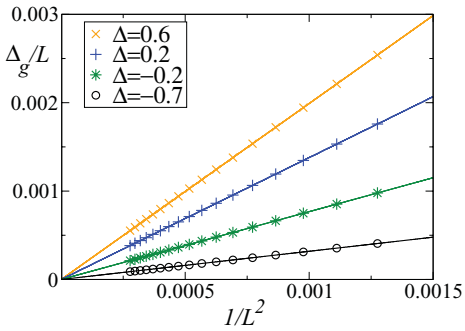

FIG. 3. (Color online) Finite-size scaling of the energy gap Δ_g as a function of $1/L^2$ for different values of Δ; solid lines are best fits (see text). The Luttinger parameter estimated via Eq. (7) is, from top to bottom, $K = 2.44(0), 2.95(9), 3.69(4), 6.03(1)$.

As one way to estimate K, we make use of the previously calculated v_s and apply the level spectroscopy method by targeting the first excited state with total magnetization $\langle \sum_i S_i^z \rangle = 1$ under PBC. Given its energy density $\epsilon_{+1}(L)$, the energy gap $\Delta_g(L) = L[\epsilon_{GS}(L) - \epsilon_{+1}(L)]$ scales to zero in the thermodynamic limit as[10,29]

$$\Delta_g(L) = \frac{\pi v_s}{2KL} + \cdots. \tag{7}$$

We thus performed a least-square regression fit as a function of $1/L^2$ and a nonlinear fit of the form $\Delta_g(L) = b_0/L^2 + b_1/L^{b_2}$ in order to estimate the effect of higher-order corrections, which turns out to be negligible if $|\Delta| \leqslant 0.9$, as can be inferred from typical finite-size scalings shown in Figs. 3 and 4. At the antiferromagnetic point, however, the quality of the best fit with just algebraic contributions turns out to be insufficient due to the presence of strong logarithmic corrections.[41] We thus apply the same fitting procedure of Ref. 39, which takes into account logarithmic corrections as ensuing from the underlying SU(2) Wess-Zumino-Novikov-Witten field theoretical structure,[9,42] obtaining $K = 0.499 \pm 0.005$ at the critical point, in good agreement with previous numerical[39] and analytical findings.[12] A summary of the so-obtained results

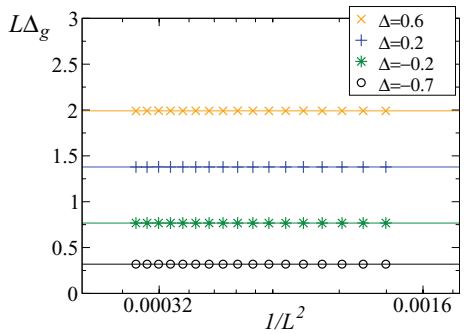

FIG. 4. (Color online) Finite-size scaling of the rescaled energy gap Δ_g as a function of $1/L^2$ (in logarithmic scale) for the same anisotropies considered in Fig. 3: solid lines are best fits (see text), showing how additional finite-size contributions are usually negligible.

over all the critical regime is presented in Fig. 8 and will be discussed at the end of this section.

The second way of estimating K is the one introduced by the authors in Ref. 30, based on the finite-size corrections of the bipartite Rényi entropies:

$$S_\alpha(l,L) = \frac{1}{1-\alpha}\log_2 \mathrm{Tr}_A\, \rho_A^\alpha \tag{8}$$

whose scaling, for a CFT with $c = 1$, follows:[35]

$$S_\alpha(l,L) = \frac{c\left(1+\frac{1}{\alpha}\right)}{6\eta}\log_2[L\,\sin(\pi l/L)/\pi] + s_\alpha + S_\alpha^{\mathrm{osc}}(l,L), \tag{9}$$

where for $\alpha \to 1$ one recovers the von Neumann entropy (4). The influence of the Luttinger parameter on such entanglement entropies is encoded in the oscillating factor, which on a finite chain of size L scales as[29,30,35]

$$S_\alpha^{\mathrm{osc}}(l,L) = \cos(2k_F l + \omega)\frac{f_\alpha\left(\frac{l}{L}\right)}{\left|2\,\sin k_F\frac{\eta L}{\pi}\,\sin\frac{\pi l}{L}\right|^{2K(L)/\eta\alpha}}, \tag{10}$$

where $k_F = \pi/2$ is the Fermi momentum and $f_\alpha(l/L)$ is a scaling function.[35] In order to circumvent finite-size corrections to the central charge and nonuniversal features related to f_α, one can consider the following entropy difference:

$$dS_\alpha(L) = S_\alpha\left(\frac{L}{2},L\right) - S_\alpha\left(\frac{L}{2}-\frac{\pi}{2k_F},L\right), \tag{11}$$

which for $L \gg 1$, reduces to[30]

$$dS_\alpha(L) = \frac{\pi^4\left(1+\frac{1}{\alpha}\right)}{48\eta\,\ln 2k_F^2}\frac{1}{L^2} + \frac{\cos(k_F L)}{L^{2K/\eta\alpha}}\left[a + O\left(\frac{1}{L}\right)\right]. \tag{12}$$

The finite-size scaling of dS_α with respect to the system size L allows one to precisely estimate K under both OBC and PBC, as discussed in detail in Ref. 30.[47] Since it has been noticed that the oscillation amplitude is very small for Heisenberg chains with $S > 1/2$ and $\alpha \simeq 2$, we employed REs with larger values of α in order to get a reliable estimate from the DMRG results. In particular, our estimates of K are mostly based on the $\alpha = 10$ RE, as these data represent a good compromise between small oscillation amplitude and slow oscillation decay.[48]

Typical results from both PBC and OBC with system sizes $L \in [28,60]$ ($L \in [100,180]$) are presented in Figs. 5 and 6. We notice that even though it considerably decreases close to the ferromagnetic transition, the magnitude of the oscillation is still large enough to perform accurate finite-size scaling. For $\Delta > 0$, comparable results may be obtained even with smaller α's. However, close to the antiferromagnetic point, different types of corrections arise and the quality of the fitting procedure rapidly decreases. Thus, extracting K beyond $\Delta = 0.7$ turns out to be numerically challenging. As can be seen from Fig. 8, data points obtained via dS_α significantly deviate (with about a 5%–15% discrepancy) from other estimates in this regime. Finally, let us point out that, for $\Delta = -0.9$, the decay exponent for PBC is so large that oscillations are strongly dumped for large system sizes, so that an accurate estimate of K is not possible; for OBC instead, being the exponent smaller by a factor of 2, the estimate is still in very good agreement with all other methods, even for $\Delta = -0.9$.

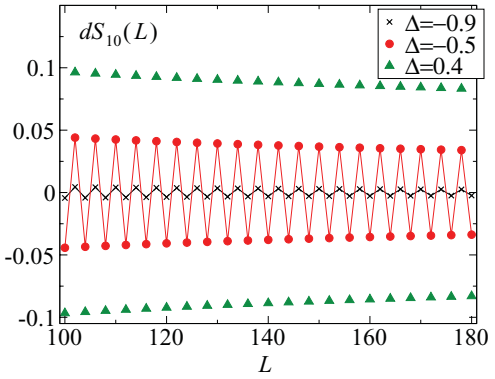

FIG. 5. (Color online) Oscillating factor of the $\alpha = 10$ RE as a function of the system size L for OBC. The amplitude of the oscillations strongly decreases when approaching the ferromagnetic point (Ref. 36), even though an accurate estimate of K is still possible (with typical relative error around 10^{-2}) by considering the appropriate entanglement entropy.

The third way we estimate K is through spin fluctuations.[43] For a bipartition as the one used to define the von Neumann entropy, we define the quantity $F = \langle(\sum_{i\in A} S_i^z)^2\rangle - \langle\sum_{i\in A} S_i^z\rangle^2$. For a TLL under PBC, spin fluctuations behave as[10,30,43]

$$F(l,L) = \frac{K}{\pi^2}\ln\left[\frac{L}{\pi}\sin\left(\frac{\pi l}{L}\right)\right] + A_1 + O(l^{2K}) \tag{13}$$

and provide a quantitative estimation of K.[30,43,44] We employ such method by fitting the half-lattice spin fluctuation $F(L/2,L)$ as a function of the system size in the interval $L \in [28,60]$; typical fitting results are illustrated in Fig. 7. At the antiferromagnetic point $\Delta = 1$, logarithmic corrections to correlation functions severely modify Eq. (13): strong oscillations, not captured by a quadratic TLL theory, emerge with respect to the parity of L, preventing a reliable estimate of K.

The results obtained in this section are all shown in Fig. 8, from which one can see that they agree over almost the whole anisotropy parameter range. In general, the level spectroscopy method leads to more accurate estimates, as the quantities

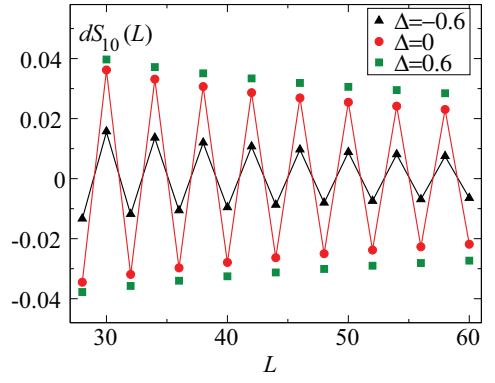

FIG. 6. (Color online) Oscillating factor of the $\alpha = 10$ RE as a function of the system size L for PBC. Continuous lines are guides for the eye.

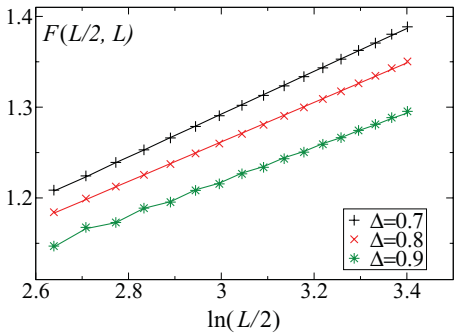

FIG. 7. (Color online) Spin fluctuations as a function of the system size L under PBC. Solid lines are best fits with Eq. (13).

it relies on are very accurately estimated with DMRG, and additional finite-size corrections seem to play a minor role; on the contrary, RE estimates, which are extremely precise for $\Delta < 0.6$, may indeed suffer from both larger truncation errors and stronger finite-size dependences close to the antiferromagnetic point, resulting in a worst mutual agreement with fluctuations and LS. Finally, all results are compared with a previously stated conjecture based on exact calculations on small system sizes[38] which relates the Luttinger parameter K_S of a spin-S Heisenberg chain with the $S = 1/2$ case in the $\Delta < 0$ regime:

$$K(\Delta)_S = 2SK(\Delta)_{1/2}. \tag{14}$$

Remarkably, as can be seen from Fig. 8, this conjecture appears to be in semiquantitative agreement with the numerical results even well beyond its original validity regime. Discrepancies among the results emerge mainly close to the antiferromagnetic point, where logarithmic corrections differently affect

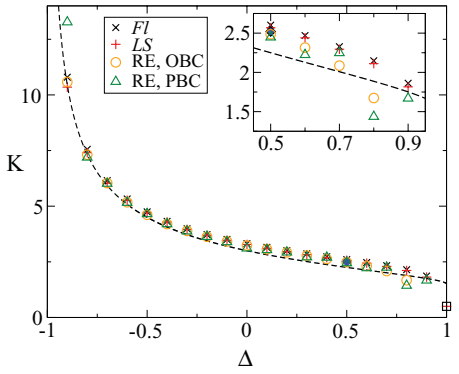

FIG. 8. (Color online) Estimate of the Luttinger parameter as a function of the anisotropy parameter. In the legend, Fl, LS, and RE denote spin fluctuations, level spectroscopy, and RE results with OBC or PBC. The dashed line is the conjecture of Ref. 38. The blue diamond ($\Delta = 0.5$) and the black square ($\Delta = 1$) indicate the LS and exact results given in Refs. 29 and 12, respectively. The inset shows a magnification of the region close to the antiferromagnetic point: here, REs do not provide fully reliable results due to the presence of additional finite-size corrections, while predictions from LS and spin fluctuations are in excellent agreement. In both panels, numerical errors are smaller than the size of the symbols, except for the $\Delta = -0.9$ estimate based on RE with PBC: in this case, the absolute numerical error due to the fitting procedure is of order 2 due to a very strong size dependence of the fits.

the techniques we have presented: in this regime, level spectroscopy turns out to be the most reliable method to extract the Luttinger parameter, as field theoretical instruments allow one to perform a more accurate scaling hypothesis with respect to methods based on REs and fluctuations. Nevertheless, the picture suggests that a deeper theoretical insight on the analytical properties of both REs and fluctuations close to critical point with logarithmic corrections may, in principle, enlarge their regime of applicability.

IV. NUMERICAL RESULTS: ENTANGLEMENT ENTROPIES AND CONNECTION WITH CFTs

A. Rényi entropies of excited states

In recent times, an analytical formula for the REs of low-energy excited states in a CFT was derived and numerically verified for various quantum spin chains.[45,46] In particular, it has been predicted that the trace of the reduced density matrix $\rho^{\alpha}_{A,\Upsilon}$ of excited states generated by primary operators Υ of conformal weights $h,\bar{h}$ satisfies the following relation:

$$\alpha^{2\alpha(h+\bar{h})}\,\mathrm{Tr}_A\,\rho^{\alpha}_{A,\Upsilon} = \frac{Z(\alpha)}{Z(1)^{\alpha}}\frac{\left\langle\prod_{j=0}^{\alpha-1}\Upsilon(2\pi j/\alpha)\Upsilon^{\dagger}(2\pi(j+l)/\alpha)\right\rangle_{\mathrm{cy}}}{\langle\Upsilon(0)\Upsilon^{\dagger}(2\pi l)\rangle^{\alpha}_{\mathrm{cy}}}. \tag{15}$$

Here, α is assumed to be a positive integer, but the result can be analytically continued all $\alpha \geqslant 1$; $Z(\alpha)$ is the partition function on a torus of dimensions $2\pi\alpha$ and $2\log_2[L/\pi\,\sin(\pi l/L)]$; $\langle\cdots\rangle_{\mathrm{cy}}$ denotes the expectation value on the vacuum state on a cylinder of length 2π. In particular, if Υ is a vertex operator, formula (15) predicts that the VNE (and, up to oscillating terms, all REs) of the excited state generated by Υ should be equal to the one of the ground state. This finding has been numerically verified in a series of exactly solvable spin models in Refs. 45 and 46. In order to further strengthen it, we considered the REs of the state generated by applying a vertex operator on the ground state (which belongs to the $S^z_{\mathrm{tot}} = \sum_{j=1}^{L} S^z_j = 0$ sector) thus obtaining the ground state in the $S^z = 1$ sector. Spanning the entire critical region and employing PBC, we found excellent agreement with the CFT prediction for both von Neumann and $\alpha > 1$ REs. In the former case, the entropy of excited and ground states coincide within numerical uncertainty up to a constant shift of order 10^{-2}, as can be seen from typical data presented in the upper panel of Fig. 9; for small systems up to $L = 12$, we further checked this behavior with exact diagonalization.

We afterward checked the relation between the oscillation corrections and the Luttinger parameter as extracted in the previous section by considering REs with $\alpha > 1$. Even in this case, the agreement with the predicted behavior is remarkable, except at the ferromagnetic point where the quality of the fit significantly decreases. Results of $S^{\mathrm{ex}}_{\alpha}(l,60)$ as a function of l are plotted in Fig. 9, lower panel, and suggest that the amplitude of the oscillations follows a similar behavior as in the ground-state case, namely, oscillations are more pronounced when approaching the antiferromagnetic point.

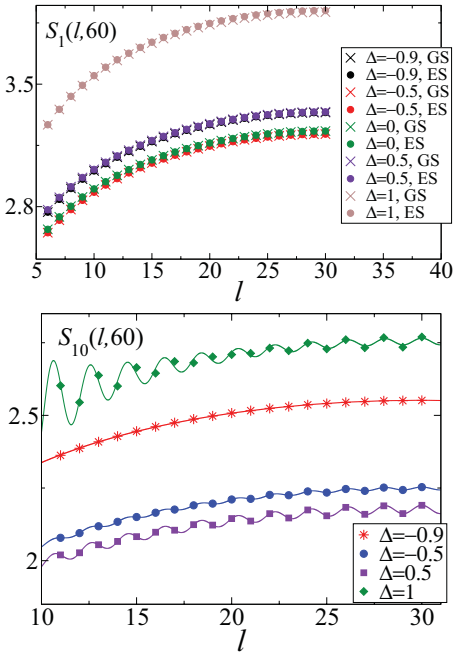

FIG. 9. (Color online) Upper panel: von Neumann entropies of ground and excited states for several values of Δ as a function of the block length l; here, $L = 60$ and PBC are considered. Lower panel: $\alpha = 10$ Rényi entropies of excited states at $L = 60$. Solid lines are best fits obtained using Eq. (10) with $k_F = 31\pi/60$.

B. Entanglement behavior of Heisenberg chains with different S

In a recent paper (Ref. 29), an interesting property concerning entanglement entropies of XXZ chains was conjectured. Based on numerical DMRG simulations, it was shown that, under both OBC and PBC, the von Neumann entropy of XXZ spin chains with different half-odd integer $S \geqslant 5/2$ satisfies the following relation:

$$(\ln 2)\Delta S_1(S) \equiv S_1(l,L)_S - S_1(l,L)_{S-1} = \frac{1}{2S-1} + \epsilon_S, \tag{16}$$

where $\epsilon_S \to 0$ in the $L \to \infty$ limit. Such relation implies that, independently on the anisotropy Δ, the nonuniversal constant contribution acquires a universal form; interestingly, it scales as the inverse of the difference between the one-site Hilbert-space dimension of the S case minus the $S = 1/2$ one.

We systematically investigated the behavior of $\Delta S_1(3/2)$ as a function of Δ by employing PBC in order to get rid of the oscillation contribution, which, as noticed in literature[36] and confirmed in the previous section, is extremely different for different values of S. As a preliminary check, we compared our value of $\Delta S_1(3/2)$ at $\Delta = 1/2$ with the one reported in Ref. 29, finding indeed very good agreement up to the different logarithmic basis employed here. Due to a very slight l dependence of $\Delta S_1(3/2)$, we mostly considered its mean value in the interval of block length $l \in [11,29]$ in systems with up to $L = 60$ sites. A schematic plot of the entropy difference at $L = 58$ is presented in Fig. 10: $\Delta S_1(3/2)$ displays a notable nonmonotonic Δ dependence. Similar plots are obtained with different L. In summary, our results firmly confirm that Eq. (16) does not hold for $S = 3/2$, in accordance with Ref. 29.

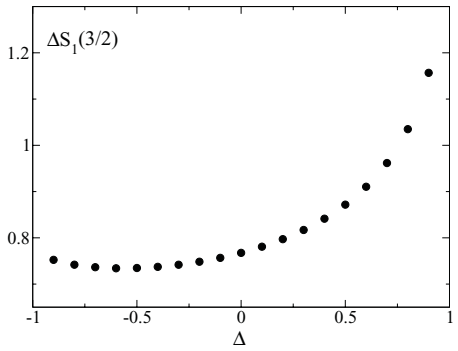

FIG. 10. Δ dependence of $\Delta S_1(3/2)$.

V. CONCLUSIONS

In this work, we analyzed critical and entanglement properties of the spin-3/2 anisotropic XXZ chain. By means of DMRG simulations, we systematically calculated the sound velocity and the Luttinger parameter in the entire critical region with a variety of methods such as level spectroscopy, entropy analysis, and spin fluctuations. At the antiferromagnetic point, logarithmic corrections prevent an accurate estimate of the Luttinger parameter via spin fluctuations and entropy oscillations, while level spectroscopy, where such corrections may be systematically introduced, still provides reliable results. Such findings benchmark the use of level spectroscopy techniques, which stem as preferable over correlation function methods based on fluctuations and Rényi entropies when approaching and determining phase transition points with logarithmic corrections. Away from such delicate regimes, all methods give compatible results, in agreement with previous studies, although REs usually require more accurate calculations since their absolute value is very small in our case study.

Finally, we investigated in detail the behavior of Rényi entropies of both ground and excited states. In the former case, we compared the REs of the $S = 1/2$ and $S = 3/2$ cases, proving that they are not connected by general relations as in the $S > 3/2$ case. Then, we provided evidence that recent results on the RE of certain excited states in a conformal field theory are verified in the model of interest, presenting the first numerical evidence of such expected behavior in nonintegrable models. Even though the leading corrections to REs of excited states and those of the ground state display the same type of behavior,[31,46] whether the combination of the two may allow for a precise determination of physical quantities of interest still stands as an open question.

ACKNOWLEDGMENTS

We thank F. C. Alcaraz, S. Evangelisti, M. Ibanez, F. Ravanini, and G. Sierra for fruitful discussions, F. Ortolani for help with the DMRG code, and G. Ramirez for technical support. This work was supported in part by the INFN COM4 Grant No. NA41. M.D. acknowledges support by the European Commission via the integrated project AQUTE.

*marcello.dalmonte@uibk.ac.at
†luca.taddia2@gmail.com

[1] W. Heisenberg, Z. Phys. **49**, 619 (1928).
[2] H. Bethe, Z. Phys. A **71**, 205 (1931).
[3] M. Takahashi, *Thermodynamics of One-Dimensional Solvable Models* (Cambridge University Press, Cambridge, 1999).
[4] A. A. Belavin, A. M. Polyakov, and A. B. Zamolodchikov, Nucl. Phys. B **241**, 333 (1984).
[5] P. Di Francesco, P. Mathieu, and D. Sénéchal, *Conformal Field Theory* (Springer-Verlag, New York, 1997).
[6] S. I. Tomonaga, Prog. Theor. Phys. **5**, 544 (1950).
[7] J. M. Luttinger, J. Math. Phys. **4**, 1154 (1963).
[8] F. D. M. Haldane, Phys. Rev. Lett. **47**, 1840 (1981).
[9] A. O. Gogolin, A. A. Nersesyan, and A. M. Tsvelik, *Bosonization and Strongly Correlated Systems* (Cambridge University Press, Cambridge, 1998), and references therein.
[10] T. Giamarchi, *Quantum Physics in One Dimension* (Oxford University Press, Oxford, 2003).
[11] I. Affleck and F. D. M. Haldane, Phys. Rev. B **36**, 5291 (1987).
[12] H. J. Schulz, Phys. Rev. B **34**, 6372 (1986).
[13] S. Itoh, K. Kakurai, Y. Endoh, and H. Tanaka, Physica B: Cond. Matt. **213**, 161 (1995); **214**, 161 (1995).
[14] H. Mutka, C. Payen, and P. Molini, Europhys. Lett. **21**, 623 (1993).
[15] A. Friedenauer, H. Schmitz, J. T. Glueckert, D. Porras, and T. Schaetz, Nat. Phys. **4**, 757 (2008).
[16] K. Kim, M.-S. Chang, S. Korenblit, R. Islam, E. E. Edwards, J. K. Freericks, G.-D. Lin, L.-M. Duan, and C. Monroe, Nature (London) **465**, 590 (2010).
[17] J. Barreiro, M. Müller, P. Schindler, D. Nigg, T. Monz, M. Chwalla, M. Hennrich, C. F. Roos, P. Zoller, and R. Blatt, Nature (London) **470**, 486 (2011).
[18] A. Micheli, G. Brennen, and P. Zoller, Nat. Phys. **2**, 341 (2006).
[19] I. Bloch, J. Dalibard, and W. Zwerger, Rev. Mod. Phys. **80**, 885 (2008).
[20] A. V. Gorshkov, S. R. Manmana, G. Chen, J. Ye, E. Demler, M. D. Lukin, and A. M. Rey, Phys. Rev. Lett. **107**, 115301 (2011).
[21] M. Dalmonte, M. Di Dio, L. Barbiero, and F. Ortolani, Phys. Rev. B **83**, 155110 (2011).
[22] J. Schachenmayer, I. Lesanovsky, A. Micheli, and A. J. Daley, New J. Phys. **12**, 103044 (2010).
[23] G. Vidal, J. I. Latorre, E. Rico, and A. Kitaev, Phys. Rev. Lett. **90**, 227902 (2003).
[24] L. Amico, R. Fazio, A. Osterloh, and V. Vedral, Rev. Mod. Phys. **80**, 517 (2008).
[25] S. R. White, Phys. Rev. Lett. **69**, 2863 (1992).
[26] U. Schollwöck, Rev. Mod. Phys. **77**, 259 (2005).
[27] S. Nishimoto, Phys. Rev. B **84**, 195108 (2011).
[28] A. Läuchli and C. Kollath, J. Stat. Mech. (2008) P05018.
[29] J. C. Xavier, Phys. Rev. B **81**, 224404 (2010).
[30] M. Dalmonte, E. Ercolessi, and L. Taddia, Phys. Rev. B **84**, 085110 (2011).
[31] J. C. Xavier and F. C. Alcaraz, Phys. Rev. B **85**, 024418 (2012).
[32] C. Holzhey, F. Larsen, and F. Wilczek, Nucl. Phys. B **424**, 443 (1994).
[33] P. Calabrese and J. Cardy, J. Stat. Mech. (2004) P06002.
[34] P. Calabrese and J. Cardy, J. Phys. A: Math. Theor. **42**, 504005 (2009).
[35] P. Calabrese, M. Campostrini, F. Essler, and B. Nienhuis, Phys. Rev. Lett. **104**, 095701 (2010).
[36] J. C. Xavier and F. C. Alcaraz, Phys. Rev. B **83**, 214425 (2011).
[37] F. D. M. Haldane, Bull. Am. Phys. Soc. **27**, 181 (1982); Phys. Lett. A **93**, 464 (1983); Phys. Rev. Lett. **50**, 1153 (1983).
[38] F. C. Alcaraz and A. Moreo, Phys. Rev. B **46**, 2896 (1992).
[39] K. Hallberg, X. Q. G. Wang, P. Horsch, and A. Moreo, Phys. Rev. Lett. **76**, 4955 (1996).
[40] I. Affleck, J. Phys.: Condens. Matter. **1**, 3047 (1989).
[41] G. Fáth, O. Legeza, P. Lajkó, and F. Iglói, Phys. Rev. B **73**, 214447 (2006).
[42] A. M. Tsvelik, *Quantum Field Theory in Condensed Matter Systems* (Cambridge University Press, Cambridge, 2003).
[43] H. F. Song, S. Rachel, and K. Le Hur, Phys. Rev. B **82**, 012405(R) (2010).
[44] S. Rachel, N. Laflorencie, H. F. Song, and K. Le Hur, Phys. Rev. Lett. **108**, 116401 (2012).
[45] F. C. Alcaraz, M. I. Berganza, and G. Sierra, Phys. Rev. Lett. **106**, 201601 (2011).
[46] M. I. Berganza, F. C. Alcaraz, and G. Sierra, J. Stat. Mech. (2012) P01016.
[47] Notice that in the limiting cases where no oscillations are present, such method cannot be trivially applied (Ref. 31). However, in the context of spin chains in Luttinger liquid regimes, a finite k_F usually ensures the applicability of such criterion (Refs. 30 and 36).
[48] A large value of α requires larger system sizes to get a reliable estimate of the oscillation decay exponent.